Large Angle Scattering of Negative Pions in Aluminum, Copper, and Lead

HARRY H. HECKMAN AND L. EVAN BAILEY
Radiation Laboratory, Department of Physics, University of California, Berkeley, California
(Received May 25, 1953)

The total cross sections for backscattering of 32±10 Mev negative pions in Al, Cu, and Pb have been measured. A stripped emulsion was embedded in a semi-infinite absorber, and exposed to an incident beam of π^- mesons. The positions and direction of mesons stopping in the emulsion were recorded. The cross sections are proportional to the ratio of the backward flux to incident flux, both of which are observed on the same strip of emulsion. The conclusions of this investigation are: (a) the scattering is consistent with energy independence in the region of 32±10 Mev; (b) the angular distribution has a maximum at 180°; (c) the cross section for backscattering is proportional to the mass number A. The total nuclear backscattering cross sections (elastic and inelastic) for negative pions in Al, Cu, and Pb are 59.6±11 mb, 192±27 mb, and 577±80 mb, respectively.

I. INTRODUCTION

ONE of the most direct ways to gather information on the nature of the pion-nucleon interaction is to study the magnitude and angular distribution of pion scattering by nuclei. Previous experiments investigating the scattering of π^- mesons by nuclei have included measurements of total and differential scattering cross sections from hydrogen[1–4] and heavier elements.[5–9] Some of the earliest information about the negative pion-nuclei interaction was obtained by the use of nuclear track emulsions.[10–15] The pion energies for these experiments have been between 30 and 150 Mev.

The present experiment studies the large angle scattering of negative pions of about 30 Mev in pure substances. The method does not differentiate between elastic and inelastic scattering, but does exclude star formation and charge exchange in the calculation of the scattering cross sections, which attenuation experiments do not. The method is adaptable most easily to elements that have a large stopping power, which precludes the use of the very light elements. For this reason, we have chosen for our study the elements aluminum, copper, and lead.

[1] Chedester, Isaacs, Sachs, and Steinberger, Phys. Rev. **82**, 958 (1951).
[2] Shutt, Fowler, Miller, Thorndike, and Fowler, Phys. Rev. **84**, 1247 (1951).
[3] Anderson, Fermi, Long, Martin, and Nagle, Phys. Rev. **85**, 934 (1952).
[4] Anderson, Fermi, Nagle, and Yodh, Phys. Rev. **86**, 793 (1952).
[5] R. L. Martin, Phys. Rev. **87**, 1052 (1952).
[6] Camac, Corson, Littauer, Shapiro, Silverman, Wilson, and Woodward, Phys. Rev. **82**, 745 (1951).
[7] A. M. Shapiro, Phys. Rev. **83**, 874 (1951).
[8] Byfield, Kessler, and Lederman, Phys. Rev. **85**, 718 (1952).
[9] Byfield, Kessler, and Lederman, Phys. Rev. **86**, 17 (1952).
[10] H. Bradner and B. Rankin, Phys. Rev. **80**, 916 (1950).
[11] H. Bradner and B. Rankin, Phys. Rev. **87**, 547 (1952).
[12] Bernardini, Booth, Lederman, and Tinlot, Phys. Rev. **80**, 924 (1950).
[13] Bernardini, Booth, Lederman, and Tinlot, Phys. Rev. **82**, 105 (1951).
[14] Bernardini, Booth, and Lederman, Phys. Rev. **83**, 1075 (1951).
[15] Bernardini, Booth, and Lederman, Phys. Rev. **83**, 1277 (1951).

II. EXPERIMENTAL METHOD

The experimental arrangement, Fig. 1, was placed on a cart and rolled through a port into the tank of the 184-inch synchrocyclotron. The π^- mesons were produced in a $\frac{1}{4}$-inch×$\frac{1}{4}$-inch beryllium target and separated from the positively charged particles by the magnetic field. The distance between the target and the scatterer-absorber established an energy spectrum for the negative pions that had a minimum energy cutoff

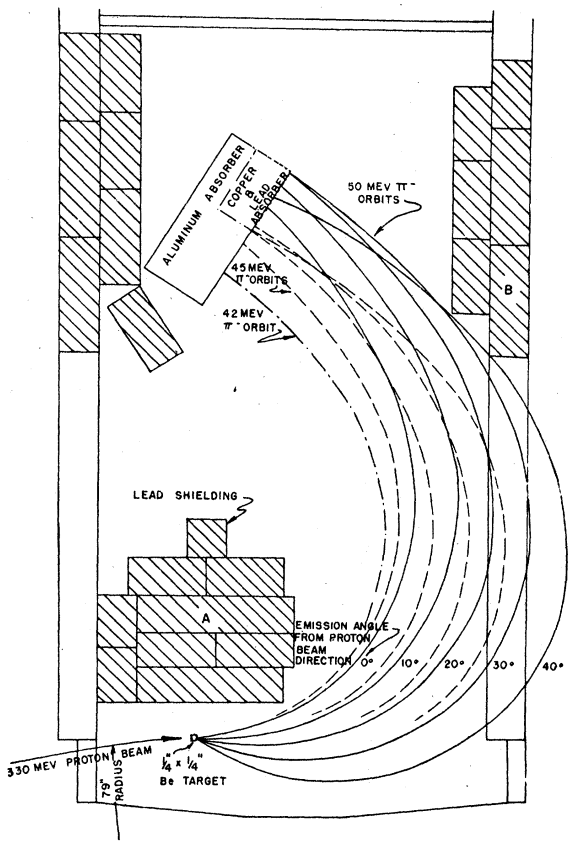

FIG. 1. Schematic drawing of experimental arrangement. Several typical π^- meson orbits of 42, 45, and 50 Mev leaving the Be target at 0 to 40 degrees from the proton beam are shown.

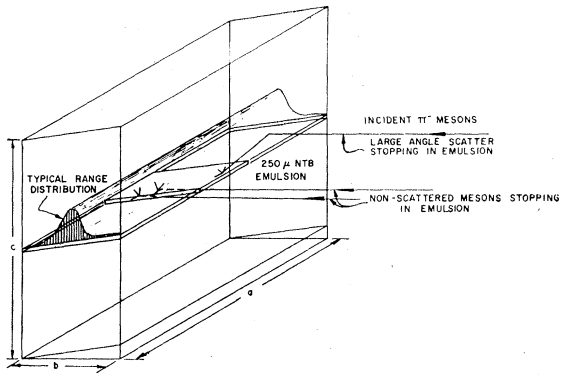

FIG. 2. Isometric sketch of aluminum absorber-scatterer showing principle of detection of large angle scattered π^- mesons.

at 42 Mev. Suitable arrangement of the lead shielding allowed no energy greater than 70 Mev to reach the scatterer regardless of the angle of emission from the target.

Figure 2 is an isometric sketch of the aluminum absorber which shows schematically how the incident flux and large angle scatters are detected. Most of the incident π^- mesons, upon entering normally to the surface of the scatterer, lose energy by ionization and come to rest after traversing a range appropriate to their energy. A small fraction of the incident mesons will suffer a nuclear interaction, such as a large angle scatter, and will come to rest at smaller depths of penetration. To sample the distribution of π^- endings, a 250 micron NTB stripped nuclear emulsion is embedded in the scatterer. The figure gives an example of an incident particle that has suffered a large angle scatter and has stopped in the emulsion. Also shown are two examples of nonscattered particles coming to rest in the emulsion at their appropriate ranges. To insure that the mesons traverse the absorber, rather than the emulsion, before entering and stopping in the emulsion, the plane of the emulsion is tilted $7\frac{1}{2}$ degrees from the perpendicular to the scatterer face. After the scattering assembly was placed in the meson beam, the stripped emulsion was removed and developed with Kodak D:19 developer and fixed. After washing, the emulsion was mounted on glass plates to facilitate scanning.

After leaving the target, mesons could possibly scatter from parts of the cyclotron, cart, or shielding, and arrive at the scatterer with reduced energies. To exclude this background, only mesons that were observed to enter the emulsion at angles greater than 90° to the direction of the incident meson beam were used to evaluate the scattering cross sections. An unknown amount of μ^- meson contamination was expected from the decay of π^- mesons while in flight. For this reason, only meson endings in both the forward and backward flux that resulted in nuclear stars were classified as negative pions.

III. THEORETICAL DISTRIBUTION OF BACKSCATTERED PIONS ENDING IN A SEMI-INFINITE ABSORBER

A particle of total range R enters normally to the absorber at 0 and scatters, elastically or inelastically, at x_1, in an interval dx_1, between θ and $\theta+d\theta$. The ending is observed between x and $x+dx$ (Fig. 3). The number of backscattered mesons that can be expected to stop between x and $x+dx$ is given by

$$D(x)dx=2\pi nNdx\int_{f=0}^{f=1}\pi(f)df\int_{90°}^{180°}\frac{\sigma(\theta)\sin\theta}{1-f\cos\theta}d\theta, \quad (1)$$

for $R<R_{\min}$. The range of a pion with an energy of about 42 Mev, the lower energy limit of the incident flux, defines $R_{\min}$. Multiple small angle scattering and range straggling are neglected, although the effect of multiple small angle scattering upon the experimental data will be considered in Sec. IV. N = the number of incident pions; $\sigma(\theta)$ = the differential cross section for

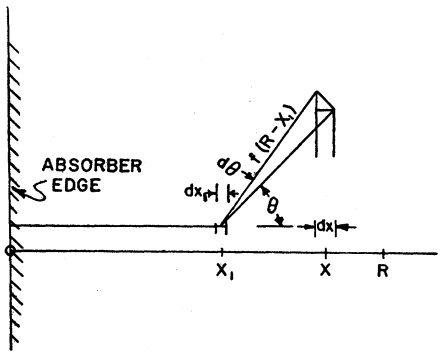

FIG. 3. Geometrical model of scattering used in theoretical analysis.

backscattering; f = the fraction of the residual range $(R-x_1)$ retained after scattering (this describes the inelastic scattering); $\pi(f)df$ = the probability that f lies between f and $f+df$; and n = the density of scattering centers.

If $\pi(f)$ and $\sigma(\theta)$ are energy independent, the integrals of Eq. (1) are independent of x, and $D(x)dx$ is a constant. The distribution can then be written as:

$$D(x)dx=kNn\sigma dx, \quad (2)$$

where

$$k=\int_{f=0}^{1}\pi(f)df\int_{90°}^{180°}\frac{K(\theta)\sin\theta}{1-f\cos\theta}d\theta, \quad (3)$$

and $\sigma(\theta)=\sigma/2\pi K(\theta)/2\pi$. $K(\theta)$ is a function of θ only, and σ is the total cross section for backscattering. k can be interpreted as the probability that a backward scattered meson will remain in the absorber, and is equal to the efficiency of the embedded emulsion for detecting backscattered mesons.

Although the contribution of inelastic scattering events is small,[10–15] the effect of inelastic scattering upon

the detection efficiency, k, is now considered. To evaluate the detection efficiency for observing inelastic backscatterers, the distribution of pion energy loss as well as the angular distribution of the inelastic scatters must be known. By studying the nuclear collisions of 60- to 90-Mev negative pions in photographic emulsions, Bernardini *et al.*[15] were able to measure the approximate initial and final energies of the inelastically scattered pions. The number of events was too small to show any definite structure in the energy loss distribution, but it was consistent with a flat distribution. The data of Lederman *et al.*[9] indicates that the angular distribution of inelastically scattered 60 Mev negative pions from carbon may be isotropic. These results form the basis for our assumptions that the probability for energy loss of inelastically scattered pions of about 30 Mev is a constant and that the angular distribution is spherically symmetric.

$P(E)dE=(\text{constant})\cdot dE$ transforms to $\pi(f)df=mf^{m-1}df$, using the empirical range-energy relation

TABLE I. The geometrical detection efficiencies for backscattered pions in a semi-infinite absorber. $\pi(f)$ describes the inelastic nuclear scattering, where f is the fraction of the residual range retained by an inelastically scattered pion. $K(\theta)$ is the angular distribution.

$K(\theta)$	$\pi(f)$	Description	Detection efficiency k[a]
any	$\delta(f-0)$	Completely inelastic, $f=0$	1.000
1	mf^{m-1}	Inelastic isotropic scattering	0.863
1	$\delta(f-1)$	Elastic isotropic scattering	0.693
$\cos^2\theta$	$\delta(f-1)$	Elastic scattering, $\cos^2\theta$ distribution	0.580

[a] Fraction of backscatters that remain in absorber.

$E_{\text{Mev}}=c(R-x_1)^m$. When m is taken as 0.60 for Al, Cu, and Pb, the detection efficiency, Eq. (3), for inelastic isotropic collisions becomes 0.863. This factor is the fraction of backscattered pions that would remain in the absorber if all scattering events were inelastic and the distribution of the energy loss is described by the function $P(E)=$constant.

Table I gives numerical values of k for several distributions of $K(\theta)$ and $\pi(f)$. In the order listed in the table, the combinations of the distributions chosen for $K(\theta)$ and $\pi(f)$ become more favorable for backscattering out of the absorber. Consequently, the fraction of backscatters that remain in the absorber decreases. This behavior is characterized by the values of k. When no particles escape the absorber, as would be expected for highly inelastic scatters, the value of k is one, the upper limit. The lower limit is 0.50. This would occur if all scatters were elastic and $\theta=180°$, since all particles of range R that were backscattered at a depth of penetration less than $R/2$ would be able to escape the absorber.

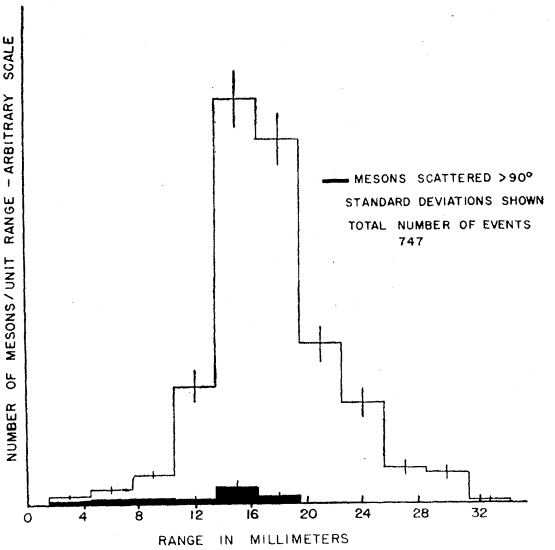

FIG. 4. Distribution of π^- stars in lead.

IV. ANALYSIS AND RESULTS OF EXPERIMENTAL DATA

The total scattering cross section is given by Eq. (2):

$$\sigma=\frac{1}{k_{\text{eff}}n}\frac{D(x)}{N},$$

where $D(x)$ is the observed number of backscatters per cm and N is the total number of particles observed in the incident flux. $D(x)$ and N are determined by scanning the nuclear emulsions from near the leading edges to the range of 70-Mev mesons in each absorber. Five to ten scans through the complete range spectrum were sufficient to determine N. The scanning effort was then turned to finding backscattered pions that stopped in the emulsion at smaller depths of penetration. The data taken for each meson ending observed were (a) depth of penetration, (b) projected angle of entrance into the emulsion, (c) approximate range in the emulsion, (d) type of ending—σ (star-forming) or ρ (non-star-forming), and (e) the number of prongs if a σ-type meson.

Figure 4 is a histogram showing a typical distribution of the pions ending in an absorber. The dark areas represent backscattered pions. Figures 5(a), (b), and (c) show the distribution of backscatters ending in the range intervals 2 to 26 mm in aluminum, 2 to 11 mm in copper, and 1.5 to 10.5 mm in lead. Figure 5(d) is the combined data for all backscatters. From geometrical consideration (employing the incident energy spectrum and the range-energy relations), the deduced scattering energies are 30.7 ± 7.0 Mev in aluminum, and 33.2 ± 8.6 Mev in copper and lead. Statistical tests applied to the spatial distributions of backscattered pions, Fig. 5, showed these distributions were consistent with a straight line of zero slope. This justifies the assumption of energy independence in the energy region of 32 ± 10 Mev in Sec. III.

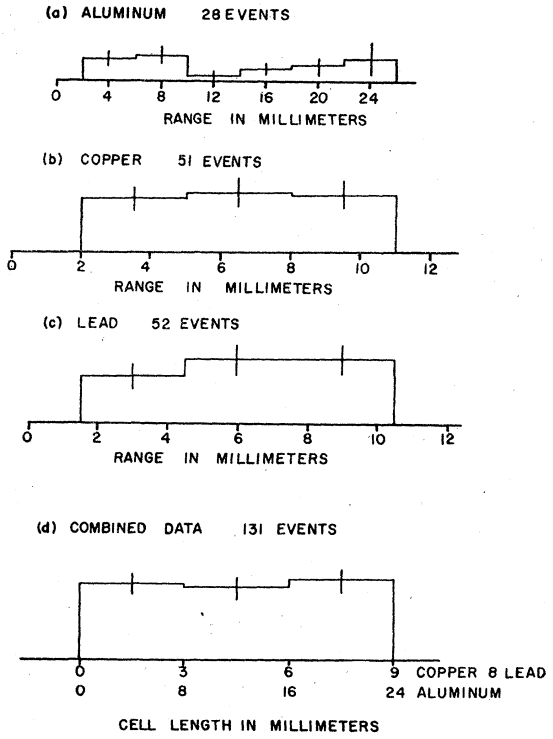

FIG. 5. Distribution of backscattered negative pion endings in aluminum, copper, and lead. Also combined data.

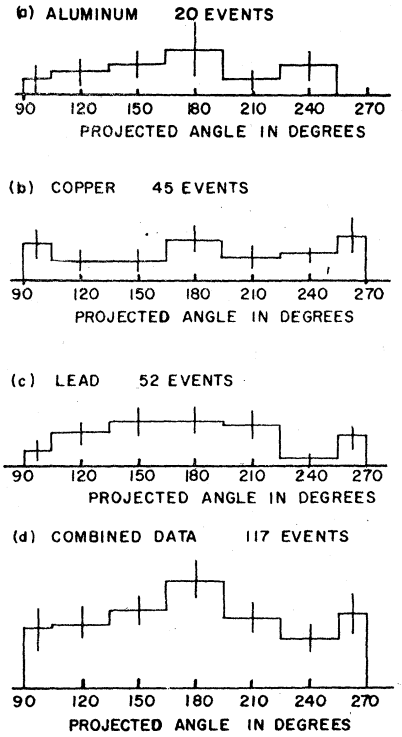

FIG. 6. Horizontal projection of entrance angles greater than 90° for negative pions into emulsion from aluminum, copper, and lead.

1. Effective Detection Efficiency

The effective detection efficiency, k_{eff}, depends upon the angular distribution of the backscattering as well as the amounts of elastic and inelastic scattering. Since the fraction of inelastic scattering present cannot be ascertained from the data, we can refer to the work of Bradner and Rankin[10,11] and Bernardini *et al.*[12–15] From their results an estimate for the fraction of inelastic

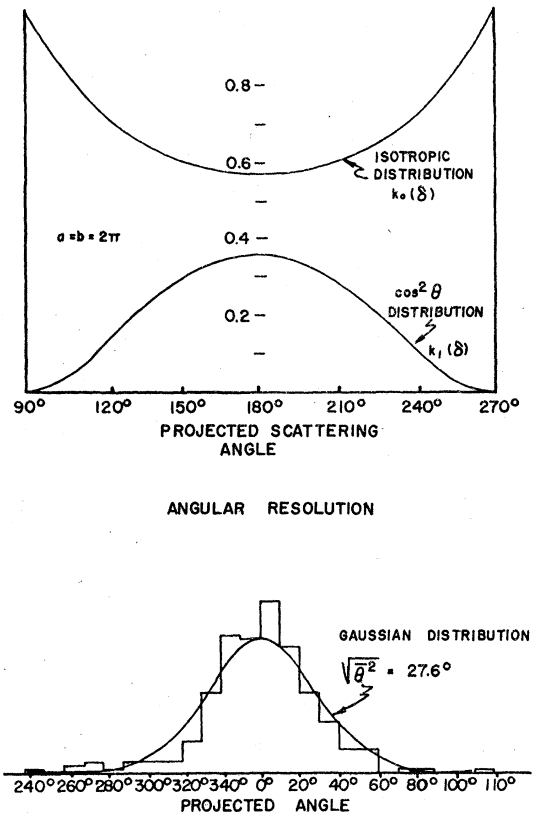

FIG. 7. (a) Horizontal projection of angular distribution, $(a+b\cos^2\theta)/(1-\cos\theta)$; (b) Angular resolution for backscattered pions.

backscattering between negative pions of about 30 Mev and complex nuclei, to one-place accuracy, is $0.2\pm0.1=\sigma_{\text{in}}/\sigma$.

Figure 6 shows the projected entrance angles of star-forming pions that entered the emulsion 90° or greater to the direction of incident flux. After eliminating the contribution of inelastic scattering to the combined angular distribution, Fig. 6(d), the coefficients a_{el} and b for elastic backscattering were determined by least squares fitting. The angular distribution for the elastically backscattered pions that stop in the embedded emulsion is, from Eq. (3), assumed to be

$$k(\theta)d\theta=\frac{(a_{\text{el}}+b\cos^2\theta)}{1-\cos\theta}\sin\theta d\theta.$$

Since a reasonable fit is obtained with the two parameters, no additional terms are used to fit the distribution empirically. To compare this angular distribution with the experimental data, $k(\theta)d\theta$ is expressed as $k(\delta)d\delta$, the projected angular distribution. When the experimental angular distribution is folded into $k(\delta)$, the theoretical angular distribution can be applied to the experimental data to determine the coefficients a_{el} and b.[16]

Figure 7(a) shows $k_0(\delta)d\delta$, the projected angular distribution which corresponds to an isotropic distribution in θ, and $k_1(\delta)d\delta$, the horizontal projection of a $\cos^2\theta$ angular distribution. The angular resolution for the backscatters, Fig. 7(b), was determined by measuring the projected entrance angles of the pions that made up the incident flux. Figure 8 is the fold of the distribution $k_0(\delta)$ and $k_1(\delta)$ and the experimental angular resolution. A least squares analysis of the data gives the best fit when $b=5.54\pm2.4a_{el}$. The fractions of the backscattered pions that contribute to the following modes of scattering are thus:

(1) $0.2\pm0.1=a_{\text{in}}$ for isotropic inelastic scattering,
(2) $0.28\pm0.09=a_{\text{el}}$ for isotropic elastic scattering,
(3) $0.52\pm0.15=b/3$ for $\cos^2\theta$ elastic scattering.

TABLE II. Observed ratios of the numbers of backscattered pions per cm to the total number incident upon the aluminum, copper, and lead absorbers. The mean values are used to evaluate the total backscattering cross sections.

		Aluminum	Copper	Lead
$\frac{D(x)}{N}$	Observer A	$2.26\pm0.22\times10^{-3}$	$12.13\pm3.04\times10^{-3}$	$15.07\pm4.3\times10^{-3}$
	Observer B	2.55 ± 0.83	10.20 ± 1.72	12.64 ± 2.1
	Mean	2.33 ± 0.44	10.73 ± 1.51	13.15 ± 1.83

The value of k_{eff} is given by

$$k_{\text{eff}}=\sum \text{(probability of type of scatter) (detection efficiency)}$$
$$=a_{\text{in}}(0.863)+a_{\text{el}}(0.693)+\tfrac{1}{3}b(0.580)$$
$$=0.66\pm0.025.$$

2. Scanning Efficiencies

Table II tabulates the ratio of $D(x)/N$ obtained by the two observers. The weighted mean is used to calculate the total backscattering cross sections, Eq. (2). If the scanning efficiencies of the observers are the same for $D(x)$ and N, the ratio $D(x)/N$ obtained is the true ratio. The relative efficiencies of the observers for finding π^- stars was 75 ± 5 percent. A direct check on the relative efficiencies for finding backscatters was not possible due to the fact that these events were extremely rare. In the areas scanned for backscatters, however, there were enough low energy background particles, principally μ mesons, from which an estimate of the relative efficiencies for the detection of backscatters could be made. Within statistical limits, it was concluded that efficiencies of the observers for finding $D(x)$ and N were the same. The percentage of star forming backscatters was observed to be 72.8 ± 6.0 percent. This agrees well with the accepted value of 72.2 ± 2.0.[17] This agreement suggests that all backscatters observed were pions, and indicates also that the scanning technique was not biased towards many pronged stars.

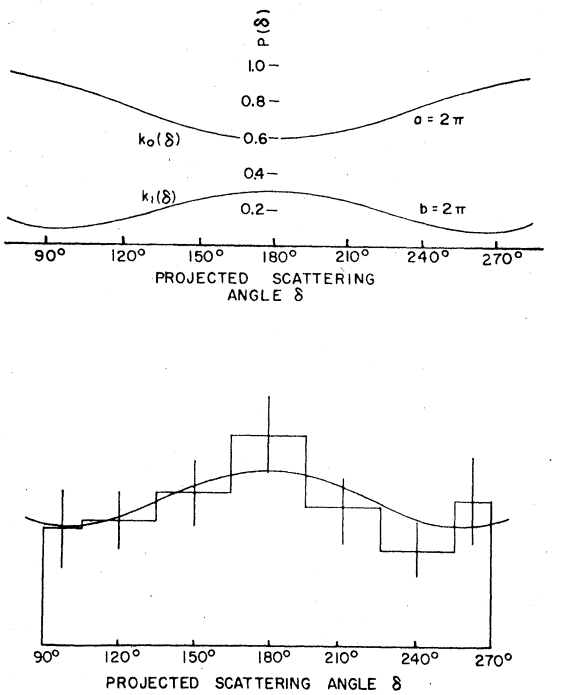

FIG. 8. (a) Folded angular distributions $k_0(\delta)$ and $k_1(\delta)$; (b) Least squares fit to experimental angular distribution.

In lead, Fig. 4, 2.3 percent of the pions detected in the incident flux, at depths of penetration greater than 13.5 mm, entered the emulsion at angles greater than 90° to the beam direction. This percentage of backscatters in the main flux is consistent with the number expected from multiple small angle scattering while the energy is degraded from 50 to 4 Mev. The correction to be applied to $D(x)/N$ for this Coulomb contamination in lead is -4.5 percent. The corrections for this effect in copper and aluminum are negligible. The correction to $D(x)/N$ for aluminum due to flux deviations at the surface of the absorber amounts to $+1.6$ percent.

3. Cross Sections

Using the effective detection efficiency, 0.66 ± 0.025, and including the above corrections, the total cross sections for large angle scattering of negative pions in aluminum, copper, and lead are as follows:
The backscattering cross sections *vs* A are plotted in Fig. 9.

[16] The fold $f(\delta)$ of the function $k(\delta)$ and $g(\delta)$ is defined by the formula $f(\delta)=\int_{-\infty}^{\infty}k(t)g(t-\delta)dt$.

[17] Frank Adelman, University of California Radiation Laboratory Report UCRL-530, 1950 (unpublished).

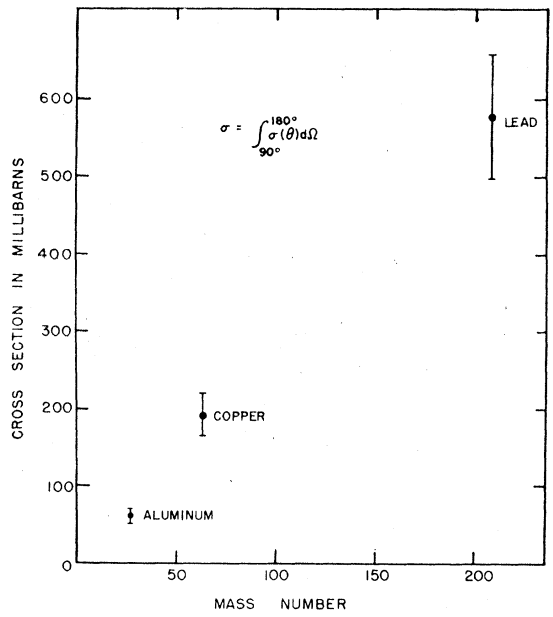

FIG. 9. Backscattering cross sections *vs* mass number A.

V. DISCUSSION

The conclusions obtained from the experimental results can be summarized as follows.

(a) The scattering of negative pions from complex nuclei is consistent with energy independence in the region of 32±10 Mev.

(b) The angular distribution for backscattering indicates that both the S and P waves contribute to the backscattering.

(c) The cross section for backscattering is proportional to the mass number, A.

The flatness of the combined data, Fig. 5(d), supports, in general, the argument for the energy independence of backscattering. If it were assumed that the energy dependence for backscattering is proportional to E^n, i.e., $\sigma(E) \sim E^n$, then the backscattered pions would be distributed as $(R-x)^{0.6n}$, where R is the total range of the particle and x is the depth of penetration. To estimate the limit of energy dependence, a least squares fit to the combined data gives for the exponent n, (-0.2 ± 0.8). Of the individual elements, aluminum is the only one in which there is an indication that the scattering may have a greater dependency upon energy. The distribution, however, is still consistent with energy independence.

Of particular interest is the indication that the cross section for backscattering may vary as A, and not as $A^{\frac{2}{3}}$. A possible interpretation of this result is outlined in the following argument. Small angle pion-nuclei scattering are collisions which, in general, involve small momentum transfers. These small angle collisions can be thought of as arising from the interactions between pions and whole nuclei since small momentum transfers correspond to large impact parameters. With the whole nucleus entering into the scattering process, one would expect the scattering cross section in this case to vary as $A^{\frac{2}{3}}$. Conversely, one must identify with large angle scattering large momentum transfers between pions and nuclei. For this to occur, the pion must approach the nucleus so closely that the interaction may now take place between the pion and a single nucleon. Under these circumstances, one may expect to observe scatters that actually arise from pion-nucleon collisions within the nucleus and, therefore, the cross section to vary as A, the number of nucleons in the nucleus.

The lowest pion energy used to study π-proton scattering has been approximately 50 Mev. At this energy the total cross sections are about 4 mb for π^- mesons[2] and 20 mb for π^+ mesons.[3] The total cross sections rise rapidly with increasing energy. In this investigation, the average backscattering cross section per nucleon, σ/A, for 32±10 Mev π^- mesons is 2.66±0.24 mb per nucleon.

The interpretation of the apparent proportional relationship between the backscattering cross sections and A as an indication of pion-nucleon collisions, while cogent, is not conclusive. It is observed that the scattering process is essentially energy independent between 20 and 40 Mev. This seems to be inconsistent with the assumption of pion-nucleon collisions, which are highly dependent upon energy. This contradiction, however, arises from the assumption that the property of strong energy dependence of pion-nucleon collisions can be extrapolated to energies below 50 Mev, well below the observed resonant scattering energy of about 150 Mev.

TABLE III. Cross sections for backscattering.

Element	σ(elastic+inelastic) $= \int_{90°}^{180°} \sigma(\theta) d\theta$ Cross section in millibarns	Cross section per nucleon, σ/A, in millibarns
Aluminum	59.6±11	2.22±0.41
Copper	192 ±27	3.00±0.42
Lead	577 ±80	2.78±0.38

The same relation between σ and A would result if the nucleus were partially transparent to low-energy pions of about 30 Mev. The observed total cross sections per nucleon for backscattering are indicative of small total interaction cross sections per nucleon for negative pions at this energy. Under these circumstances, light nuclei, such as aluminum, would be highly transparent, enabling the pion to "see" all the nucleons in the nucleus. It is surprising that the results indicate that this argument is apparently valid for the heavier elements, copper and lead. In these cases, less transparency might be expected, and the cross sections would conduce to an $A^{\frac{2}{3}}$ relationship.

We wish to express our sincere appreciation to Dr. Walter H. Barkas for his continued interest throughout the experiment. We are grateful to Professor R. L. Thornton and Dr. J. V. Lepore for their helpful comments. Finally we wish to thank Mr. J. Vale and the cyclotron crew for their aid in making the bombardments.